Office of Naval Research
Contract N00014-87-K0128

# Effects of Initial Conditions on the Development of Supersonic Turbulent Free Shear Layers



**Final Report**

Period 2/1/87 -10/31/88







February 20, 1989

D. S. Dolling and Y. R. Shau

Department of Aerospace Engineering
and Engineering Mechanics

~~University of Texas at~~ Austin

## TABLE OF CONTENTS

# 1. INTRODUCTION

## 1.1 Background

In recent years a considerable amount of attention has been focused on the development of air-space transportation systems such as the National Aero-Space Plane (NASP). One of the major research challenges is the design of a high speed, efficient propulsion system for NASP. At present, no single propulsion system can provide reasonable efficiency over the entire flight range (i.e., Mach number range from 0 to 25). Currently, the supersonic combustion ramjet (Scramjet) is considered to be the most suitable approach, at least for Mach numbers at and above the high supersonic range. The advantage of the scramjet is that it can be operated over a wider range of Mach number than other air-breathing engines. Figure 1 shows the schematic of a typical engine (from reference 1). It can be seen that the mixing process between the fuel and the air stream is controlled by supersonic shear layers.

However, many aspects of supersonic combustion are not well understood. An overview of the latter and many of the other research needs for the development of such propulsion systems for hypersonic vehicles has been recently compiled by Waltrup[1]. In the scramjet propulsion system, as the name implies, the combustion process is entirely supersonic, and proper fuel-air mixing is critical. Theoretical and experimental studies of supersonic shear layers have shown that the shear layer grows at a very slow rate, which is a problem since the fuel-air interface is bounded by the edge of the shear layer. For efficient combustion, rapid and uniform mixing of the two streams forming the shear layer is desirable. Rapid shear layer growth is also required to keep the combustor short, its weight low, and the cost low. Therefore, innovative techniques

which can substantially enhance the growth rate of supersonic shear layer are needed.

Methods to enhance the spreading rate of the shear layer would obviously be easier to develop if the mechanisms controlling its growth were known. Unfortunately, the mechanisms of turbulent mixing in supersonic free shear layers are not well understood or documented. On the other hand, there is a great deal of information and a basic understanding of the physics of incompressible shear layers. Some of the earlier experiments in compressible turbulent shear layers were conducted using free jets which have supersonic flow ($M_1>1$) on one side and zero velocity ($M_2 = 0$) on the other [2-5]. These results showed that compressible shear layers grow more slowly than incompressible shear layers, and the spreading rate decreases with the increase of Mach number. Since the total temperature and static pressure were kept equal in these experiments, it was thought that the lower spreading rate could be attributed to the density difference. Brown and Roshko[6] made a series of experiments in incompressible flow in which density differences were introduced by using different gas combinations to simulate the effect of Mach number. It was found that density has some effect on the spreading rate but it is much smaller than that observed in supersonic flows. They concluded that compressibility itself plays a critical role in supersonic shear layers.

In a more recent study conducted by Papamoschou[7], and Papamoschou and Roshko[8], an apparatus was constructed to examine the effects of varying $M_2$ from subsonic to supersonic values while keeping $M_1 > 1$. The spreading rate was correlated with a parameter called convective Mach number, $M_c$, which is based on the velocity of the moving frame in which the large-scale vortex structure is nearly

stationary (Figure 2). The stable nature of the supersonic mixing layer was demonstrated using schlieren flow visualization. It was observed that for $M_c > 1$, the shear layer spreading rate was about one-fourth of that for an incompressible shear layer at the same velocity and density ratio. The theoretical study of Bogdonoff[9], in which supersonic shear layer growth rates were correlated against a Mach number, $M^+$ (defined as the geometric average of the Mach numbers of the large structure), shows similar results (Figure 3). Generally, the trends of experimental and analytical work suggests that one of the factors contributing to the lower spreading rates with increasing $M_c$ is the decrease in the growth rates of large scale eddy structures which develop initially from the Kelvin-Helmholtz instability of the vortex sheet. However, more work is needed to confirm this.

## 1.2 Mixing Enhancement Studies

Although $M_c$ can be controlled in a laboratory environment and flow conditions may be set to provide the largest possible spreading rate, this may not be possible in a full scale engine. For a given $M_c$, which has fairly small spreading rate, mixing enhancement techniques are required.

Weidner and Trexler[10] first investigated experimentally the effects of shock wave impingement on momentum diffusion of a supersonic shear layer. Mixing between two supersonic air streams which had mean Mach numbers of 3.5 and 4.4 was studied, and the strength of oblique shock wave applied corresponded to a turning angle of 6°. Pitot pressure measurements were taken across the shear layer at several stations on either side of two crossing shock waves and were reduced to velocity profiles. The experimental results indicated a 40% increase in shear layer thickness

downstream of the shock waves when compared to the theoretical solution. However, some question remains as to whether this increase of shear layer width is a result of the shock waves or not. It might have been a natural consequence of the near-field shear layer, because no baseline(undisturbed shear layer) measurements were made.

Recently, Kumar et. al.[11] compiled a overview of mixing augmentation techniques. Their numerical study suggested that mixing enhancement can be achieved by applying oscillating shocks which introduce high frequency disturbances to the flow and enhance turbulence in the mean flow. Also, shock-wave oscillation generates fluctuation energy directly from the mean flow and becomes an excellent source for turbulence energy. It has been well demonstrated in shock wave/boundary layer interactions that perturbing a turbulent boundary layer with shock waves results in the amplification of turbulence stresses and vorticity fluctuations downstream of the interaction region.[12-13] However, little is known about the shock wave/shear layer interaction and the effects of external disturbances on the spreading rate of supersonic shear layers. Therefore, no conclusions can be drawn at the present time. Since shock waves will be unavoidable in the scramjet engine internal flow field, they may become simple and powerful tools for mixing enhancement if they can be controlled and applied appropriately. It should be noted that the generation of additional shock waves solely for the purpose of mixing enhancement may not be justified, since the tradeoff between energy losses (shock drag), combustor length reduction, and the combustion efficiency requires a great deal of consideration.

## 1.3 Objective

The long range objective of this study is to find ways, preferably mechanically simple and passive, of enhancing the spreading rate of supersonic free shear layers. The intention is to test several types of disturbances including single and multiple plane shock waves, corrugated shock waves(these are shock waves with a periodic spanwise pressure gradient), and vortex generators. In the first period of this study, described in this report, the objective was to design and build the model and air supply system, construct and validate the instruments, and then perform exploratory tests under the undisturbed and disturbed flow conditions. To determine the velocity profiles at various streamwise locations, pitot pressure, static pressure and total temperature probe surveys were made. Instrument validation tests were also performed to determine the capabilities such as uncertainty, frequency response, and repeatibility.

Preliminary results of the baseline case and shear layer enhancement using planar shock wave impingement were obtained. The shock wave was generated by using a plane wedge on the tunnel ceiling, and the shock strength was controlled by the wedge angle. The study included impinging the shock on either the upstream boundary layer(at two streamwise positions) or the shear layer. Pitot pressure profiles were measured at the last possible downstream position (i.e., 5.3" from the trailing edge of the nozzle lip) for these cases. Since the results were limited by the resources (i.e., static probe) , detailed measurements will be performed in the second period of study to confirm these preliminary findings. The experimental program and results are presented in the following sections.

## 2. Experimental Program

The experimental program was conducted at the University of Texas Wind Tunnel Laboratories located at Balcones Research Center. The wind tunnel test facility, instrumentation and test procedures are described in the following sections.

### 2.1 Test Facility

The test facility is a 7 in. by 6 in., Mach 5 blowdown wind tunnel with adjustable stagnation pressure and temperature. Tests were performed in a new test section designed for this project. A schematic view of the experimental setup is shown in Figure 4. The floor and ceiling of test section are slotted, to allow probes to be moved streamwise and spanwise with effectively infinite resolution. The slot is 6.5 in. long in the streamwise direction and is covered by rectangular aluminum plates with 6 circular plugs for the probes to go through. The probe drive is mounted on the top of the aluminum plates in a variety of positions to accommodate all plug locations. A linear variable displacement transducer (LVDT) on the probe drive is used to determine the vertical location of the probe tip.

For powering the tunnel, atmospheric air air is compressed using a Worthington 4 stage compressor and is then passed through filters to remove the air impurities, and stored in a 140 $ft^3$ tank at 2500 psig. A control valve monitored by a micro-processor regulates the flow into the Mach 5 tunnel. Before entering the tunnel, the air passes through a series of electric heaters to increase its stagnation temperature. This air supply system allows a maximum run time of approximately 70 seconds. Normally, the run time of a typical shear layer test is only of order 30 seconds.

## 2.2 Shear Layer Model

The model geometry for generating the shear layer is a flat plate with an internal converging-diverging Mach 3 nozzle, and is approximately 14 in. long, 6 in. wide and 0.75 in. thick. A exploded view of the model is shown in Figure 5. It consists of six relatively simple pieces: the leading edge, two side supports, a center piece used to turn the externally supplied air, a screen section and two (top and bottom) nozzle contours. The nozzle contours were designed using a method-of-characteristics code with a correction for the boundary layer displacement thickness effects to give a wave-free, Mach 3 exit flow. It is installed at zero angle of attack on centerline in the Mach 5 wind tunnel. Therefore, the shear layer is bounded by Mach 5 and Mach 3 flows. In the current study, both streams are air. The turbulent boundary layer on the plate external surfaces undergoes natural transition and, at the nozzle lip station, is about 0.2 inch thick. Since the Mach 3 nozzle spans the central 4 inches of the plate, the aspect ratio of the shear layer at the lip is about 20. A double screen assembly is installed in the plate to prevent large vortex structures generated by the turning vane from exiting the nozzle.

## 2.3 Air supply system for the Mach 3 nozzle

The air supply and control system for the nozzle is shown schematically in Figure 6. Since the air density at the exit is about twice that of the Mach 5 stream and the exit area is 4" by 0.75", the air system must be capable of supplying a large mass flow rate. Therefore, air was fed to the model through a 2" diameter pipe which is connected to a 500 $ft^3$ storage tank. The storage tank pressure was set at 150 psig during the tests. It is supplied by the main 2500 psig, 140 $ft^3$ storage tank used for the

tunnel supply.

For safety reasons, there are two valves and a rupture disk between the 500 $ft^3$ storage tank and the filter housing as shown in Figure 6. The series of filters are used to further clean the air of impurities. The air enters the model through slots in the sides. There are matching slots on both side walls of the wind tunnel which are covered by circular brass connectors attached to 1.5" diameter feed-pipes which "tee" into the main 2" diameter pipe. The pressure in the brass chambers is monitored by a transducer which outputs a signal to the Moore 352 control board which is software-programmable. A P.I.D. controller is used to adjust the opening of the "Cashco" control valve and match the measured pressure to the desired set-point.

## 2.4 Instrumentation

### 2.4.1 Probes

Two types of probes has been designed and built for this study; those for determining mean velocity profile measurements and those for fluctuating total pressure measurements. To determine the mean velocity profile, separate pitot pressure, static pressure and total temperature probes have been built. These are described below.

(a) Pitot probe - A fast response pitot probe was designed to measure the pitot pressure profiles. The probe design is shown in Figure 7. The probe tip is of standard design and has a rectangular opening about 0.008 in. high and 0.052 in. wide. To ensure a fast response, the pressure transducer is installed in the probe shaft. This makes it an order of magnitude faster than conventional probes (i.e. those with pressure lines leading to transducers outside the tunnel). Since the transducer is relatively close

to the probe tip, the frequency response of the probe is about 150-200 Hz. Data were taken at about 1 kHz with a probe drive speed of about 0.1" per second.

In the present study, a Kulite XCQ-062-50A series miniature transducer was installed in the probe shaft. It contains a fully active four arm Wheatstone Bridge strain gauge arrangement diffused into a silicon diaphragm. The pressure range is 0-50 psia with an overpressure capability of three times the rated pressure with no change in calibration. Nominal full scale of output is 75mv and the sensitivity is approximately 1.5 mv/psi. The outer diameter of the housing is 0.064 in. with a pressure sensing area of 0.028 in. diameter. The transducer has a combined nonlinearity and hysteresis of 0.5% best fit straight line (BFSL), repeatability of 0.1% FS, and a natural frequency of 600 kHz. Since only the mean pitot pressure is of interest, raw data were averaged using software to obtain a smooth pressure profile.

(b) Total Temperature probe - The total temperature probe is of standard design with a iron-constantan (J-type) thermocouple connected to a electronic ice-point. The probe tip has an outer diameter of 0.095 in. and uses thermocouple wire with a diameter of 0.015 in. Usually, total temperature probes for supersonic flow measurements have two or more vent holes around the sensing thermocouple. The vent ensures continuous replacement of air inside the probe. As suggested by Winkler[14], the best performance is obtained for a vent-area to entrance area ratio of 1:5. Therefore, four 0.015 dia. vent holes were drilled through the outer case as shown in Figure 8.

(c) Static probes - Accurate measurement of the static pressure through the shear layer has posed a considerable challenge. Two types of probes have been built and tested. A third type is currently under evaluation. The first is a traditional cone-cylinder probe

0.0625" in diameter with holes about 12 diameters from the cone-cylinder junction as shown in Figure 9a. Exploratory tests have shown that such a probe is very sensitive to wave interference. Any weak shock wave or expansion wave impinging on the section between the tip and the static holes causes incorrect reading of static pressure. This restricted the probe to flow regions where wave interference is not a serious problem. It was hoped that this problem might be resolved by a special probe which has a shorter distance from the probe tip to the holes. Therefore, a second probe of the same size was built based on the design of Donaldson et. al.[15]. It has a 25° half-cone tip and static holes 0.88 diameters downstream of the cone-cylinder junction (Figure 9b). Based on inviscid analysis, the probe should read 79.3% of the true static pressure over the Mach number range 1.4 to 5. However, the original design does not include the effects of Reynolds number based on the diameter of probe. Several tests were performed in the shear layer region, and the results indicated that viscous interaction is severe enough to cause a dependence on Mach number. Detailed results will be shown in section 3.

The third static probe under evaluation was designed by Pinckney[16] (Figure 9c). The original probe is very small and suitable for the present experiment. It is currently being built. This type of probe has been tested in NASA Langley's wind tunnel, and calibration is available in reference 16. This static pressure probe will be tested in the second period of this project.

Since the static pressures are on the order of 0.6 psi, a high sensitivity transducer is needed. A Kulite XCW-062-15A series miniature transducer was used. Most of the specifications are the same as the XCQ-062-50A described earlier,

including nonlinearity and hysteresis, repeatability and housing and pressure sensing area size but the pressure range is lower, 0-15 psia.. However, this transducer is more sensitive with a full scale output of 225mv and a sensitivity of 15 mv/psi. The transducer is also installed in the probe shaft, and consequently the frequency response is attenuated by the probe tubing. Since the purpose is to measure mean static pressure, this is of no consequence.

(d) Kulite probes - To measure the fluctuating stagnation pressure in the shear layers, two type of probes have been built as shown in Figure 10. Both probes have Kulite transducers in the tip itself and thus have a high frequency response. The first type of probe employs model XCQ-062-50A transducers which have an outer diameter of 0.062". The frequency response of the probe is about 50-60 KHz. The second type employs the model XCQ-030-100D transducer which has better spatial resolution by a factor of 4 (i.e. an outer diameter 0.030"), and higher frequency response ( 300KHz). Its disadvantage is that it is far more delicate and is much more sensitive to temperature changes than the larger model.

### 2.4.2 Vertical Displacement Measurement

To measure vertical displacement of the probe, a Schaevitz DC-operated linear variable differential transformer (LVDT), model 6000 HPD, was used. There are two integral parts to this mechanism: an AC operated LVDT and a carrier signal conditioning module. It has a range of ±3.0 inches with full displacement output 10V ±5%, and its sensitivity is 3.4 V/in. It has a linearity of ±0.10% full range. The LVDT is attached to a manually operated probe drive to provide the y-position signal for each probe survey.

### 2.4.3 Disturbance Generation

To determine the effects of shock wave impingement, a planar shock wave generator which is a 5° or 10° full span wedge(the wedge can be turned 180°) is used. The wedge was attached to the ceiling of the wind-tunnel, and could be adjusted up to 4" in the streamwise direction. Therefore, the shock can be made to impinge on the plate boundary layer or the shear layer further downstream. The inclined surface of the wedge is turned back parallel to the stream shortly after the tip to ensure that the expansion wave generated by the turning angle merges with the shock wave above the plate surface and no complex wave patterns are impressed on the boundary layer (or shear layer). Also care was taken in the design to make sure that the waves formed at the trailing edge of the shock generator do not interfere with shear layer in the measurement zone. Schematics of the arrangement are shown in Figure 11.

### 2.4.4 Signal Conditioning

Output from the pressure transducers was amplified by a Measurements Group Strain Gauge Signal Conditioning Amplifier, model 2311, while that from the temperature probe was amplified by a Dynamics amplifier, to provide a signal in the range 1 to 10 volts. Normally, gain settings were 1000 for the static pressure and total temperature and 200 for the pitot pressure. The signals were then filtered by a Ithaco Model 4113 filter with lowpass cutoff frequency set at 50 kHz. The filtered pressure signals or the temperature signal were digitized by the 12 bit A/D converter of the MASSCOMP minicomputer.

### 2.4.5 Test Procedure and Conditions

Total properties within the Mach 5 tunnel stagnation chamber were measured with a Setra Model 204 (0-500 psia) pressure transducer and a chromel-alumel thermocouple. The pressure of the air entering the Mach 3 nozzle in the model was monitored through the use of total pressure probes in the brass cavities located on the tunnel wall.

Since this is a new facility, the model air supply control system tuning parameters had to be determined before any measurements could be made. The tuning tests were run in two phases. The first phase consisted of setting up a second control loop (in addition to the original Mach 5 tunnel controller) to allow the Mach 3 flow to start and stabilize at approximately the same time. To avoid the expense of running the Mach 5 tunnel stream, a series of tests were made with the brass cavities on the tunnel side-walls hooked up to dummy plates with openings the same size as the throat area of the nozzle. Manual valve position, set point (the desired pressure in the brass cavity) and controller trip point (the pressure at which the controller goes into automatic mode) were changed as well as control parameters to determine the best settings.

Once the correct controller settings were obtained, the second phase of testing included hooking up the air supply to the nozzle and running both the Mach 5 and Mach 3 flows. The objective was to match the static pressure in the Mach 3 nozzle exit plane with those in the Mach 5 airstream. Static pressure and pitot pressure surveys were made across the shear layer at the nozzle exit to determine the location and angle of any shocks or expansions in case the nozzle was over- or under-expanded. Different values of the set point were used to determine the best pressure setting. Ideally, there would be no waves if the static pressures at the nozzle exit were perfectly matched and if the

trailing edge of the nozzle had infinitesimal thickness. Since the trailing edge of nozzle has a finite thickness of about 0.01", necessary for structural integrity, waves are unavoidable. Unfortunately, the first static probe (which was the only one available at the time) is reliable only in a stream without disturbances. Therefore, matching static pressures became a rather lengthy and entirely empirical process. It was done using the pitot probe , which is very sensitive to any waves in the flow field. From the measurements of pitot pressure profiles just downstream of the nozzle, wave angles could be determined. They were found to emanate from the nozzle lip. If the static pressures in both streams are matched, the wave angles should be close to the Mach angles of the streams on either side of the shear layer, and the strength of disturbances will then be minimized. This minimization process was carried out and provides the preliminary controller set point for the matching of static pressure. Flow conditions are very repeatable from test to test.

The third phase of testing was conducted after the most acceptable set point had been determined and the plate surface thoroughly polished. This phase consisted of testing the various probes at different streamwise locations and of conducting pitot surveys at 0.5 inch intervals downstream. Pitot surveys of the boundary layer on the model surface just upstream of the trailing edge were also performed. After the undisturbed baseline case had been completed, shear layer pitot pressure profile measurements were further made under the disturbances such as shock-boundary layer and shock-shear layer interferences. Details of the results and discussion are presented in section 4.

# 3 DATA ANALYSIS TECHNIQUES

## 3.1 Data Averaging

In order to determine the mean pitot and static pressure or temperature profiles, a data averaging code was developed to smooth the raw data that were taken. Recall that to obtain fast surveys, probes with high frequency response transducers were used. Although their location in the shaft reduced their their response significantly, they are still able to respond to fluctuations of order a few hundred Hertz. A "window" of specified size passes through the data and at each y location, pressure data within the window are averaged and assigned to that y location. The program is interactive and window size can be changed as deemed necessary to obtain a smooth profile. In this project, the smallest window size that provided a smooth profile was used.

## 3.2 "Least Squares" Turbulent Boundary Layer Fitting

From pitot surveys, The Van Driest II transformation was used to iteratively fit the data to the law of the wall-law of the wake profile. Boundary layer properties were determined by using the coefficients of the best fit curve. Assumptions such as constant static pressure and total temperature through the boundary layer and adiabatic wall conditions were made in the data reduction processes.

## 4. Results and Discussion

The Mach 5 boundary layer properties on the model surface were investigated using the pitot probe. Results shows that the boundary layer is fully turbulent and fits the u+ v.s. y+ theoretical curve well as shown in Figure 12. The corresponding boundary layer/ free stream properties are also tabulated in the same figure. The undisturbed shear layer evolution was also measured using the pitot probe. These data represent the reference case for comparison with those cases with shock wave disturbances. The measured pitot pressure profiles at several streamwise positions are shown in Figure 13, as are the observed wave patterns deduced from them. The effects of compression and expansion waves originating from the nozzle lip can be seen in the pitot profiles. Although the static pressure in the nozzle exit plane is matched with that of the Mach 5 stream (by adjusting the stagnation pressure of the Mach 3 flow), the expansion and compression waves cannot be eliminated. However, the strengths of these waves are very low and their angles are close to those of the local Mach waves.

The growth of the shear layer is much smaller than that observed in subsonic experiments, as expected. For this undisturbed case the shear layer grows almost linearly at a rate of 0.02" per inch in the streamwise direction. This corresponds to an edge slope of about 1.15 degree. Because of the uncertainties in defining the shear layer edge from pitot profiles combined with the small growth rate, the accuracy is limited. More information such as static pressure and total temperature profiles is needed, so that velocity profiles can be obtained. (Note: these surveys will be completed in the near future)

Exploratory studies of two types of disturbances have been made so far; a planar shock wave generated by a 10° wedge which impinged on the surface of the plate

at 1.0" and 2.5 inches upstream of the nozzle lip, and the same shock wave applied to the shear layer about 1.5 inches downstream of the lip. Both setups were discussed earlier in section 2.4.3 and shown schematically in Figure 11. For comparison with the undisturbed case, the mean boundary layer properties on the plate just upstream of the trailing edge after shock wave impingement were investigated. The u+ v.s. y+ velocity profile and the tabulated boundary layer properties are shown in Figure 14 and should be compared to Figure 12. Due to the shock wave the freestream Mach number above the shear layer decreases, and because of the shock-boundary layer interaction the momentum thickness increases, but the boundary layer velocity thickness is about the same as the undisturbed case. The outer part of the turbulent boundary layer is retarded, as indicated by the increase in the wake strength parameter.

Figure 15 shows comparisons of the boundary layer pitot pressure profiles at the nozzle lip for the undisturbed case and the case with the shock impinging at the boundary layer 2.5 inches upstream of the lip. Due to the effects of shock wave impingement, the freestream Mach number decreases and pitot pressure increases on the edge of the boundary layer.

The shear layer pitot pressure profiles at 5.3" downstream of the nozzle lip are shown in Figure 16. The pitot pressure profiles are referenced to the Mach 3 jet pitot pressure (i.e., $Pt(y) - Pt_{jet}$) and are plotted v.s. y (here y is measured relative to the lower edge of the shear layer). For the case with the shock wave impinging directly on the shear layer, there is no obvious influence on the shear layer thickness at 5.3" downstream of the lip. On the other hand, the cases with shock wave/boundary layer interaction cause an increase in the shear layer thickness. Whether it is a gradual

change or an abrupt change at some streamwise station in the shear layer still needs to be investigated. Also, for those cases where the shock wave impinges on the incoming boundary layer, the convective Mach number decreases, and it is known that the spreading rate increases with the decrease of convective Mach number. Whether this is the dominant influence, or whether it also is due to the turbulent intensity increase due to the shock wave which will enhance the mixing as well, is not clear. To determine what causes the enhancement of growth rate, further investigation is required.

## 5. SUMMARY

In this first period of investigation, a start has been made on studying the effects of initial conditions on the development of supersonic turbulent shear layers. The shear layer model and its air supply system have been designed and constructed. Tuning of the air supply control system as well as basic hardware validation were performed. Most of the required instrumentation has been designed and built. Through preliminary testing, it has been shown that all the instruments work as expected except the static pressure probe which has been redesigned twice due to the effects of wave interference and viscous interaction. Testing of the new static probe will be performed at the beginning of the second period of study.

Pitot pressure measurements of the undisturbed shear layer have been taken and documented, these results were used as a baseline for the comparison of cases with shock wave impingement. Two "types" of disturbance have been tested; those generated by shock wave/boundary layer interaction; and those caused by shock wave/shear layer interaction. In the preliminary testing, pitot pressure measurements for the shear layer with disturbance were made only at two streamwise stations. At the last measurement station, the shear layer thickness increases substantially when shock wave/boundary layer interaction occurs upstream of the nozzle lip. Qualitatively, the results indicate that the speading rate can be enhanced using planar shock wave impingement. Such results look promising for some other types of disturbance. However, in order to determine whether the change of spreading rate is due to the change of convective Mach number or the effect of shock-boundary layer interaction, and to understand the mechanism behind it, more detailed measurements and further investigation is needed. This will be the focus of the second phase of the study.

## Reference


[1] Waltrup, P. J., "Liquid Fuel Supersonic Combustion Ramjets: A Research Perspective of the Past, Present and Future," AIAA Paper 86-0158, AIAA 24th Aerospace Sciences Meeting, Jan. 6-9, 1986, Reno, Nevada.

[2] Bershader, D. and Pai, S. I., "On Turbulent Jet Mixing in Two - dimensional Supersonic Flow," Journal of Applied Physics, Vol.21, No.6, 1950, p.616.

[3] Pitkin, E. T. and Glassman, I., "Experimental Mixing Profiles of a Mach 2.6 Free Jet," Journal of Aerospace Sciences, Vol.25, No.12, 1958, pp.791-793.

[4] Channapragada, R. S., "Compressible Jet Spreading Rate Parameter for Mixing Zone Analyses," AIAA Journal, Vol.1, 1963, pp.2188-2190.

[5] Birch, S. F. and J. M. Eggers, "A Critical Review of the Experimental Data for Developed Free Turbulent Shear Layers," Free Turbulent Shear Flows, Vol. I and II - Conference Proceedings, NASA SP- 321, 1973.

[6] Brown, G. L. and A. Roshko, "On Density Effects and Large Structures in Turbulent Mixing Layers," Journal of Fluid Mechanics, vol. 64, pt. 4, 1974, pp. 775-816.

[7] Papamoschou, D., "Experimental Investigation of Heterogeneous Compressible Shear Layers," Ph.D. Thesis, California Institute of Technology, Pasadena, Dec. 1986.

[8] Papamoschou, D. and A. Roshko, "Observations of Supersonic Free Shear Layers," AIAA Paper 86-0162, AIAA 24th Aerospace Sciences Meeting, Jan. 6-9, 1986, Reno, Nevada.

[9] Bogdanoff, D. W., "Compressibility Effects in Turbulent Shear Layers," AIAA Journal, vol. 21, no. 6, June 1983, pp. 926-827.

[10] Weidner, J. P. and Trexler, C. A., "Preliminary Investigation of Momentum Diffusion Between Two Supersonic Air Streams in the Presence of Shock Waves," NASA TN D 4974, 1969.

[11] Kumar, A., Bushnell, D. M. and Hussaini, M. Y., "A Mixing Augmentation Technique for Hypervelocity Scramjet," AIAA Paper 87-1882, 1987.

[12] Hayakawa, K., Smits, A. J. and Bogdonoff, S. M., "Hot-Wire Investigation of an Un-separated Shock-Wave/Turbulent Boundary Layer Interaction," AIAA Paper 82-0985, 1982.

[13] Trolier, J. W. and Duffy, R. E., "Turbulence Measurements in Shock-Induced Flows," AIAA Journal , Vol.23, No.8, 1985, pp.1172-1178.

[14] Winkler, E. M., "Design and Calibration of Stagnation Temperature Probes for Use at High Supersonic Speeds and Elevated Temperatures," Journal of Applied Physics, Vol. 25, No.2, 1954.

[15] Donaldson, I. S. and Richardson, D. J., "A Short Static Probe with Good Incidence Characteristics at Supersonic Speed," Ministry of Technology, Aeronautical Research Council, Current Paper, C. P. No. 1099, 1970.

[16] Pinckney, S. Z., "An Improved Static Probe Design," AIAA Journal, Vol. 12, No. 4, 1974, pp. 562-563.

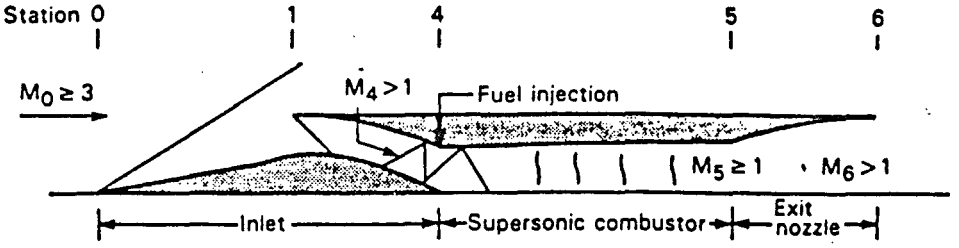


Scramjet Engine

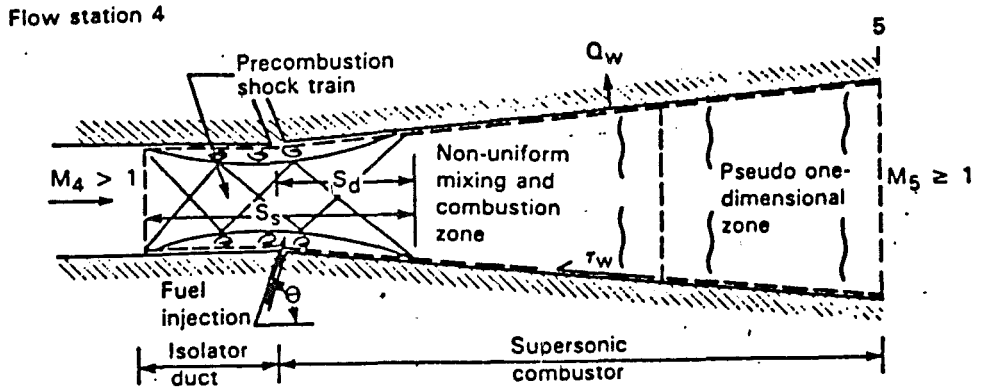


Scramjet Combustor

Figure 1. Schematic of scramjet engine (from ref. 1).

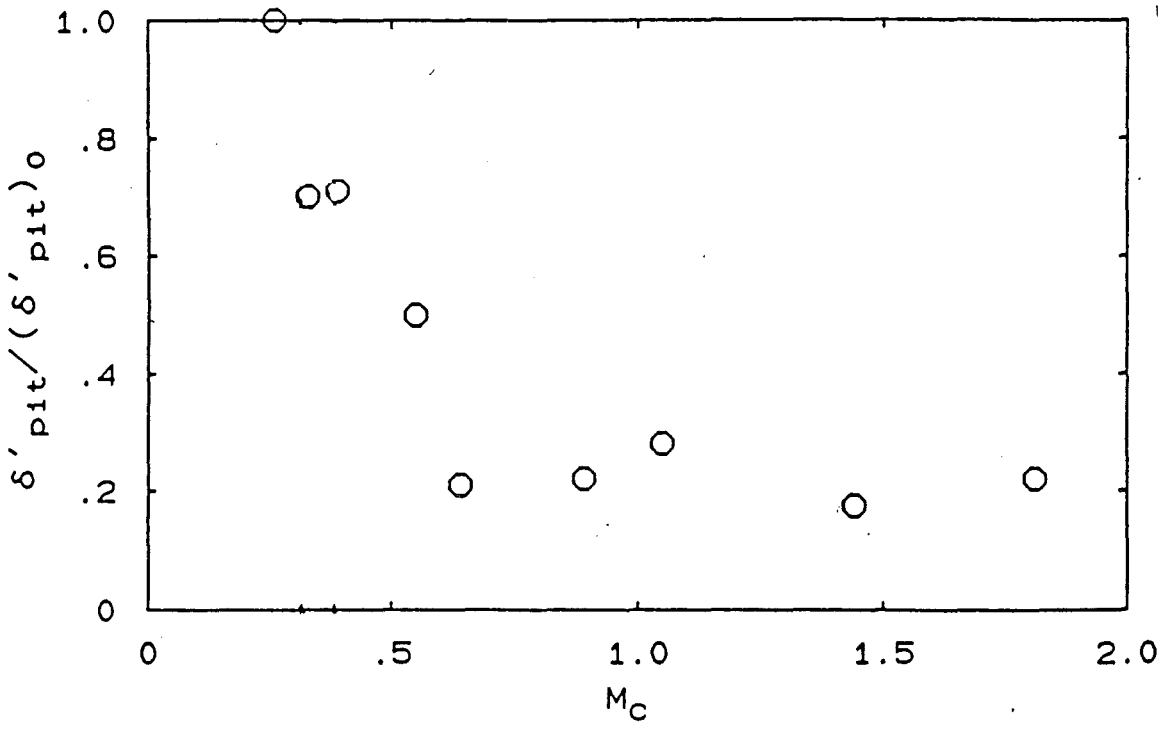


Figure 2. Effects of convective Mach number, $M_C$, on the normalized pitot thickness growth rate (from ref. 7).

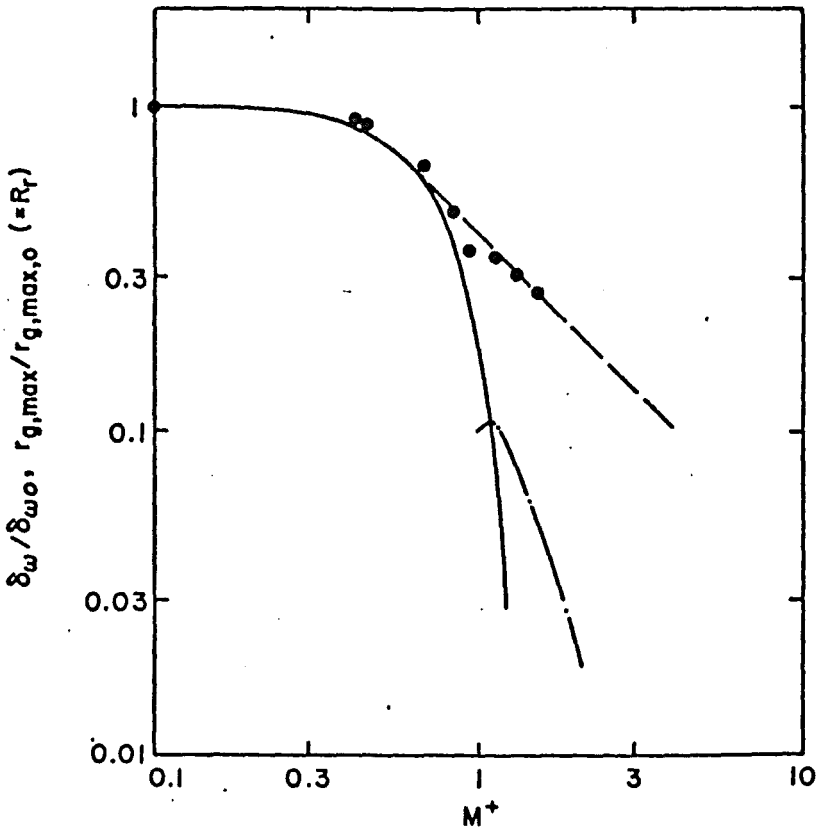


Figure 3. Effect of geometric Mach number, $M^+$, on the normalized vorticity thickness growth rate (from ref. 9).

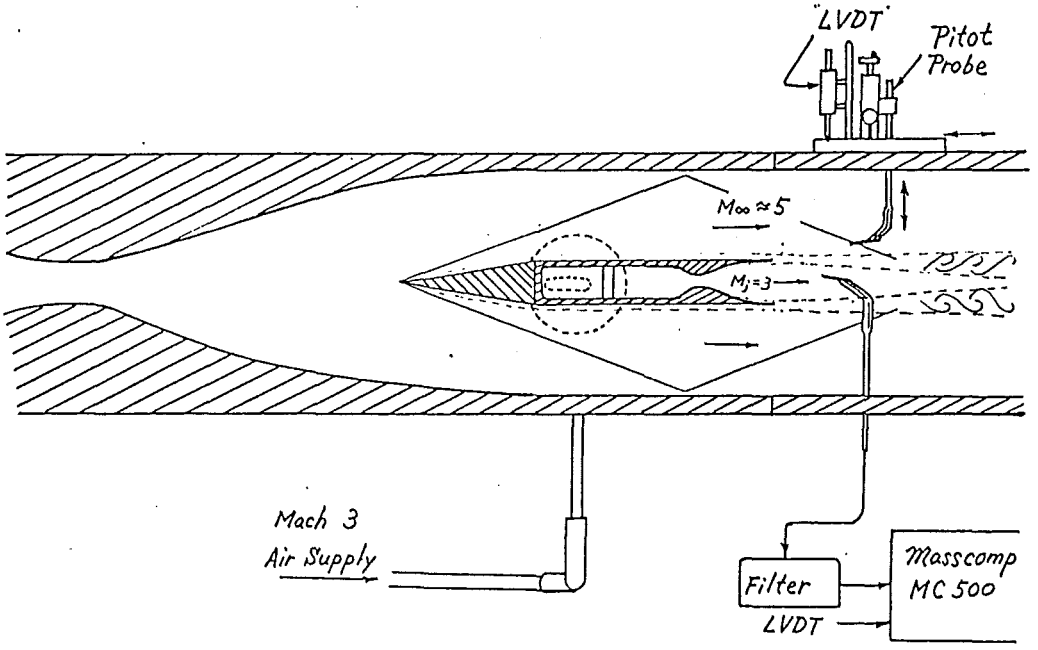


Figure 4. Schematic of experimental set-up.

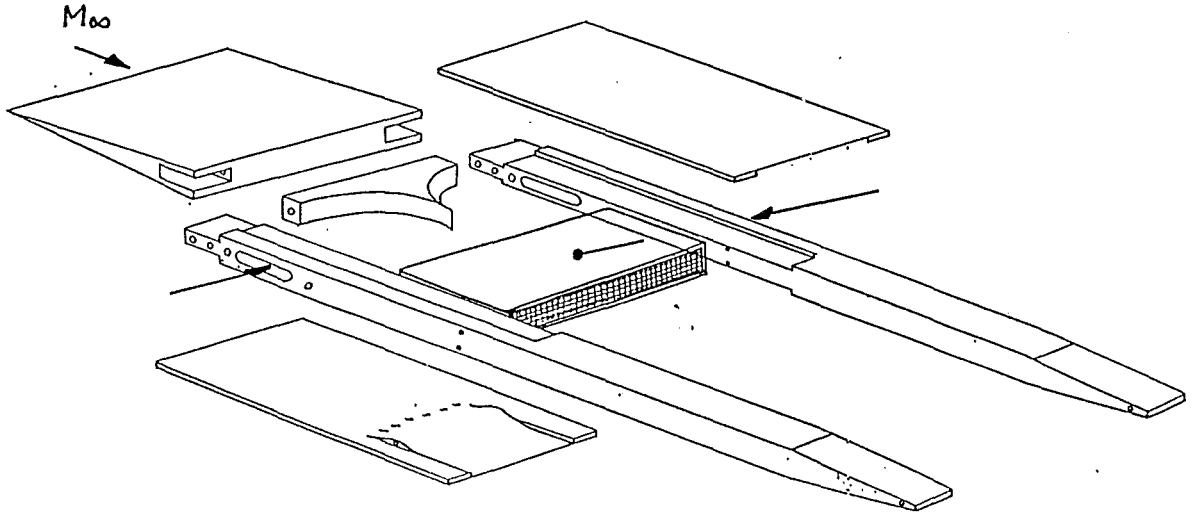


Figure 5. Exploded view of model.

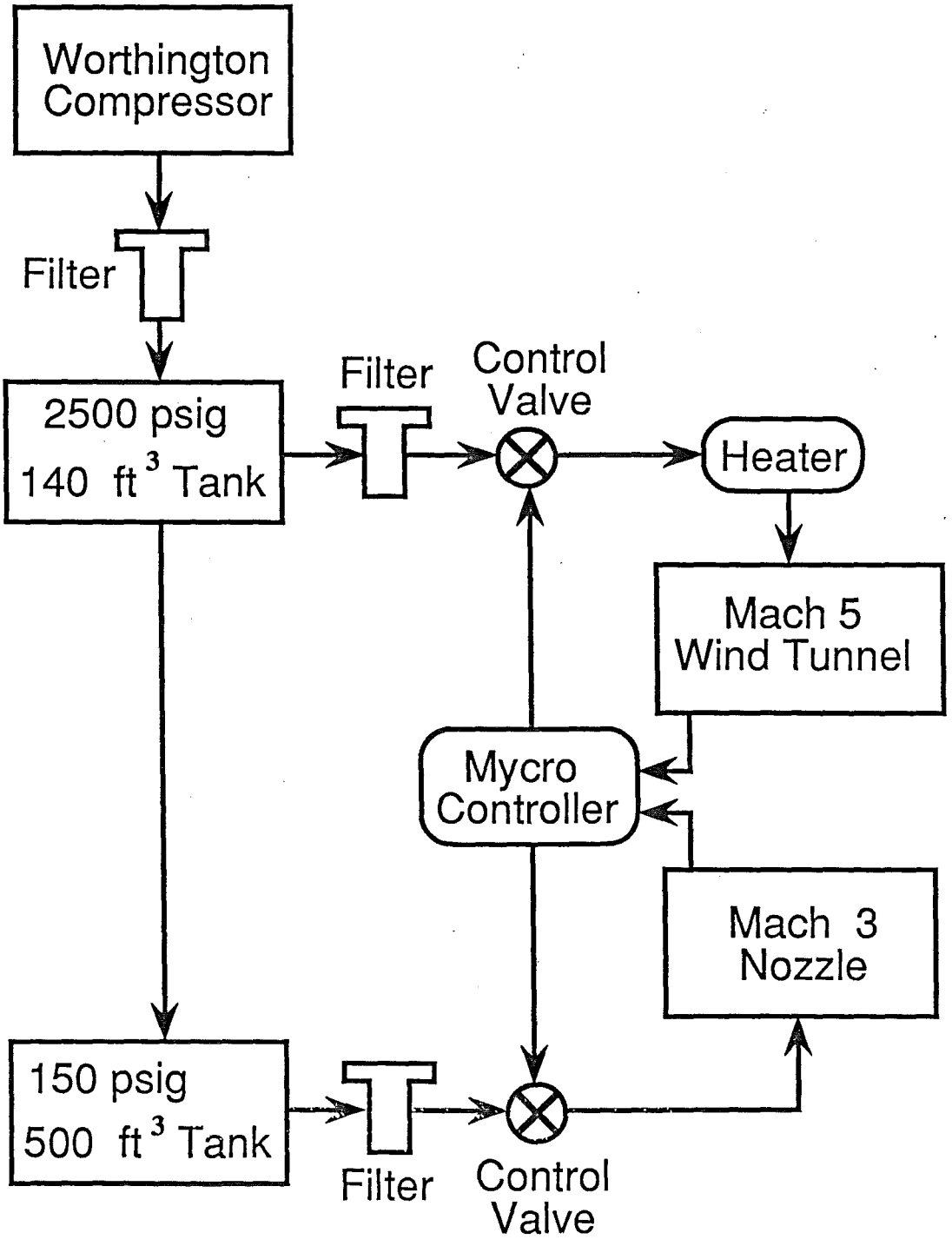


Figure 6. Schematic of air supply system.

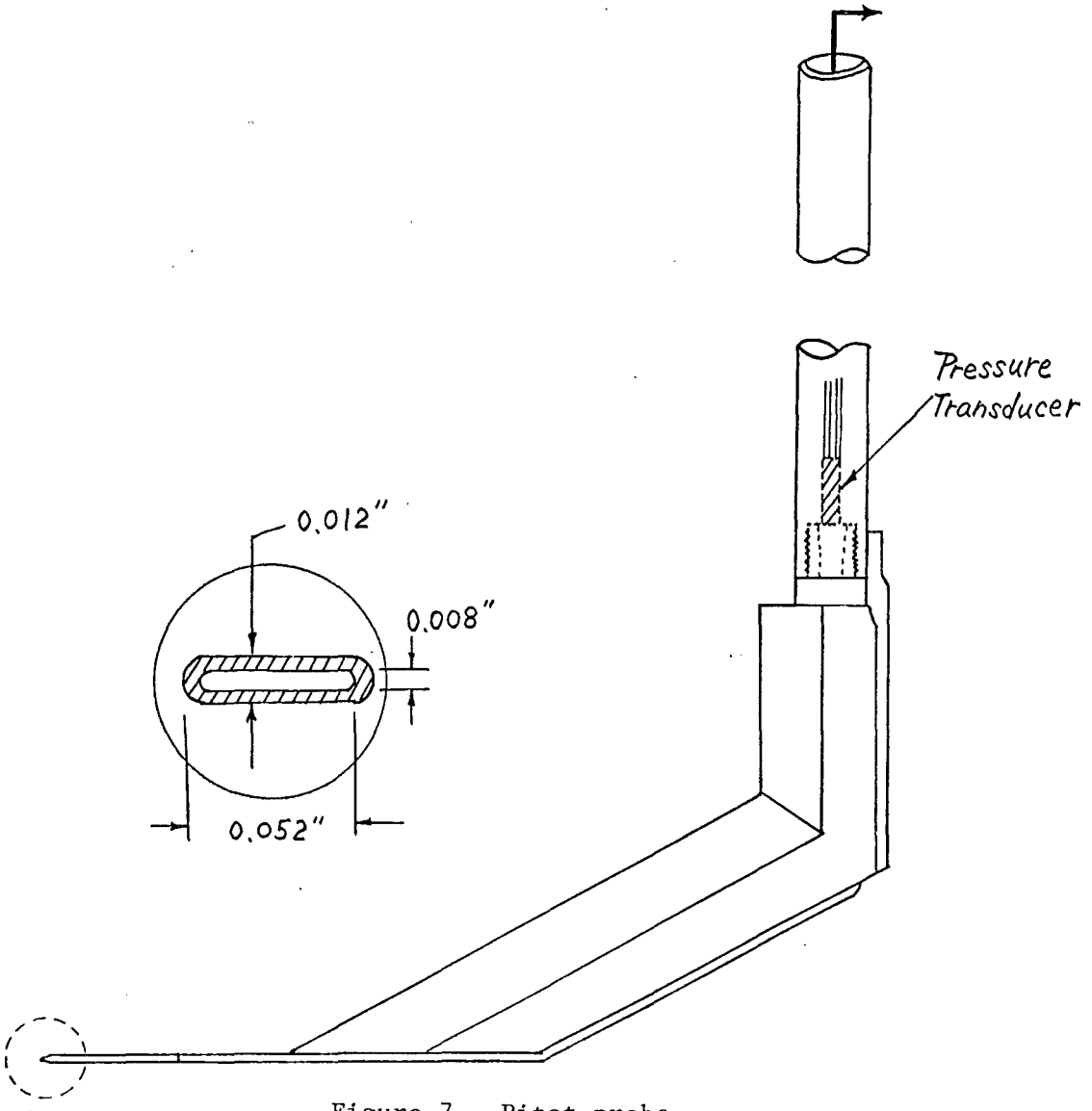


Figure 7. Pitot probe.

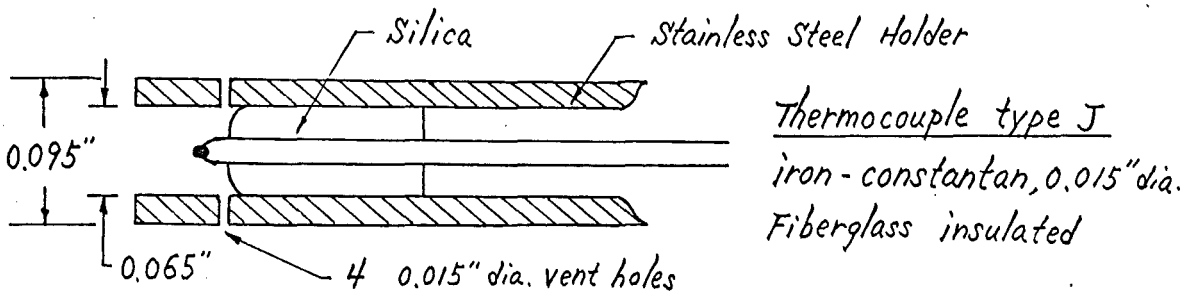


Figure 8. Stagnation temperature probe.

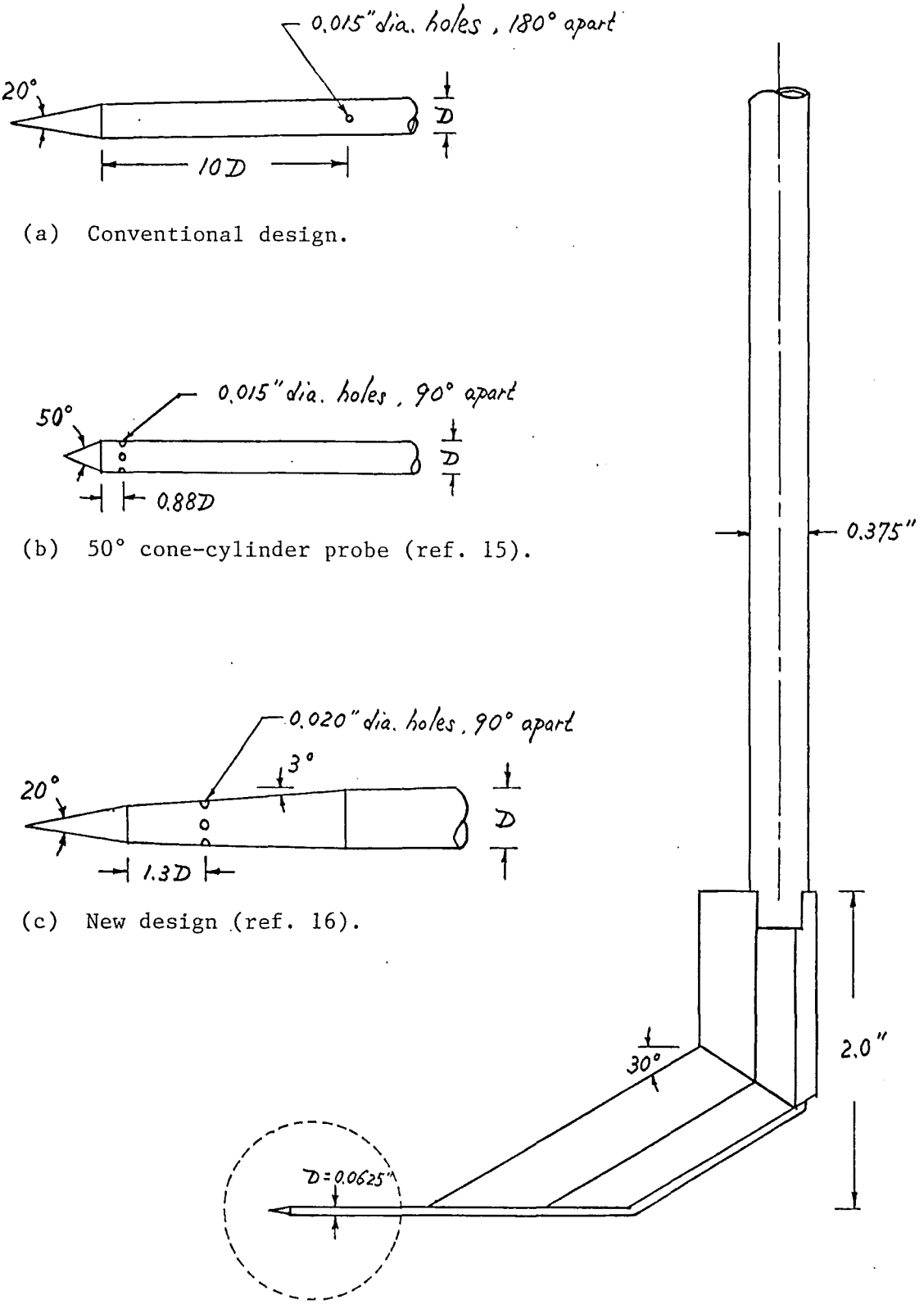


(a) Conventional design.

(b) 50° cone-cylinder probe (ref. 15).

(c) New design (ref. 16).

Figure 9. Design of static probes.

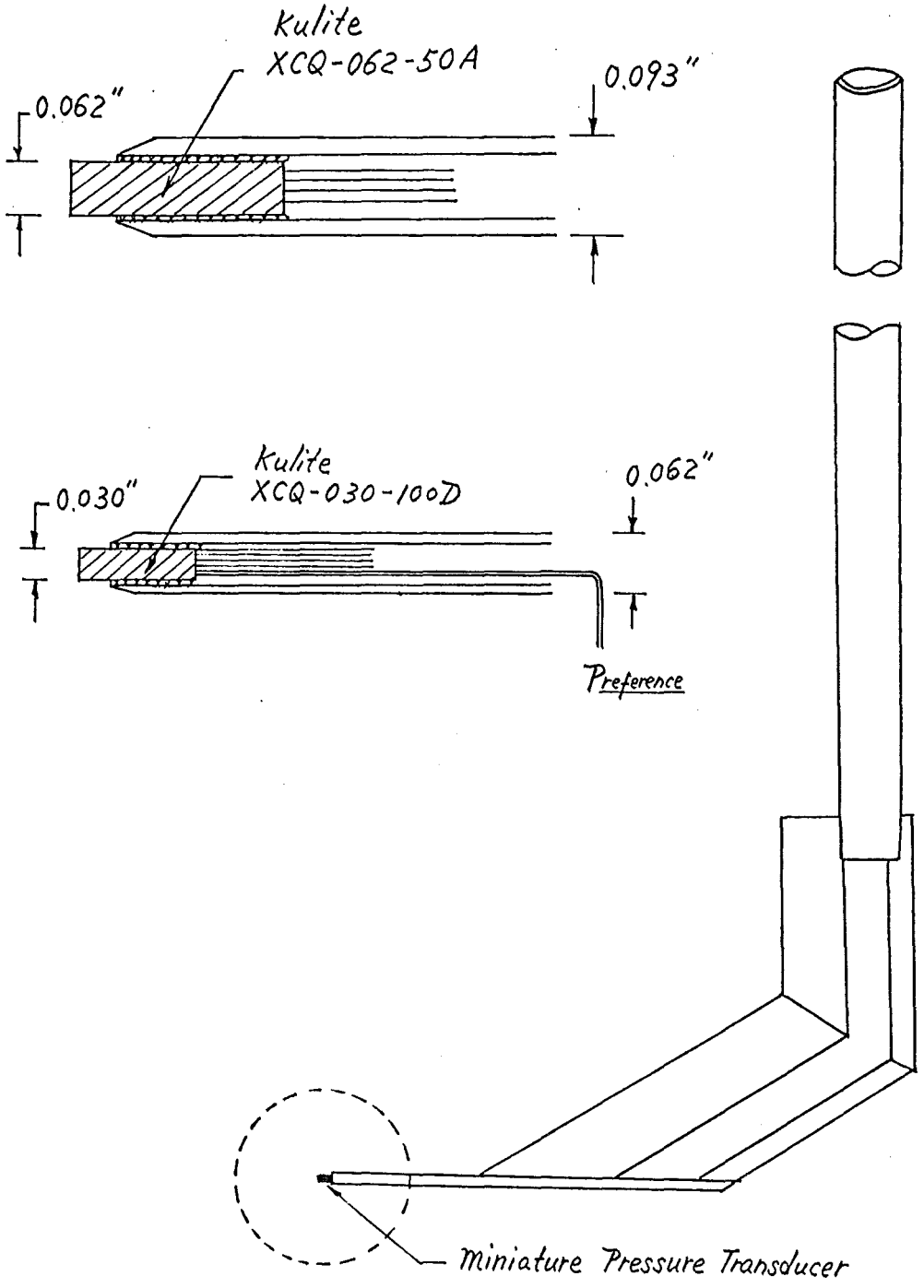


Figure 10. Kulite probes.

**Shock wave impinging on the boundary layer**

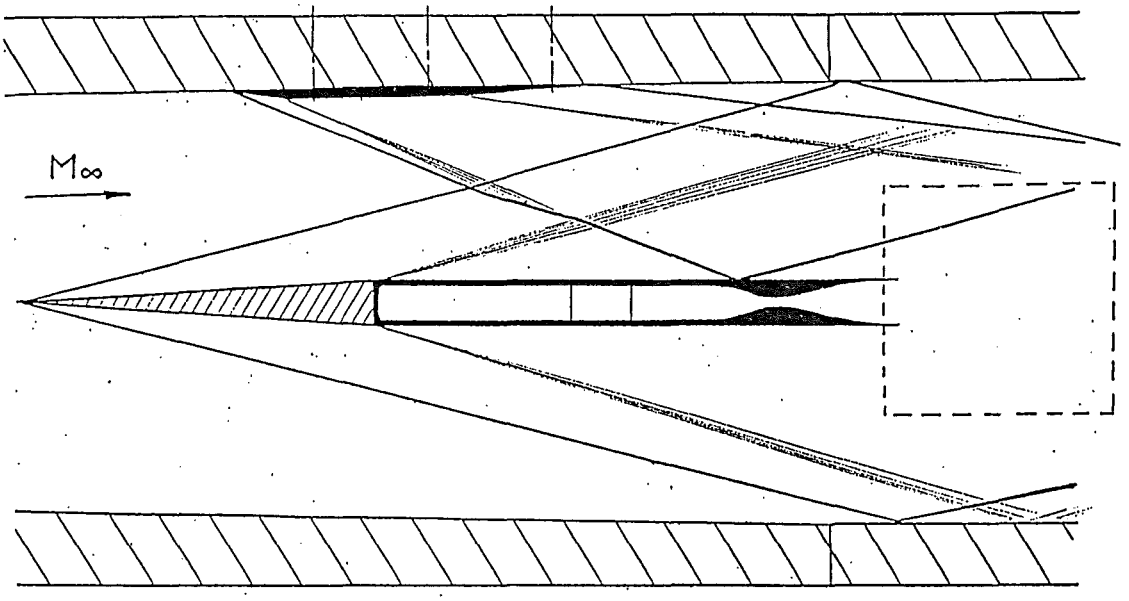


**Shock wave impinging on the shear layer**

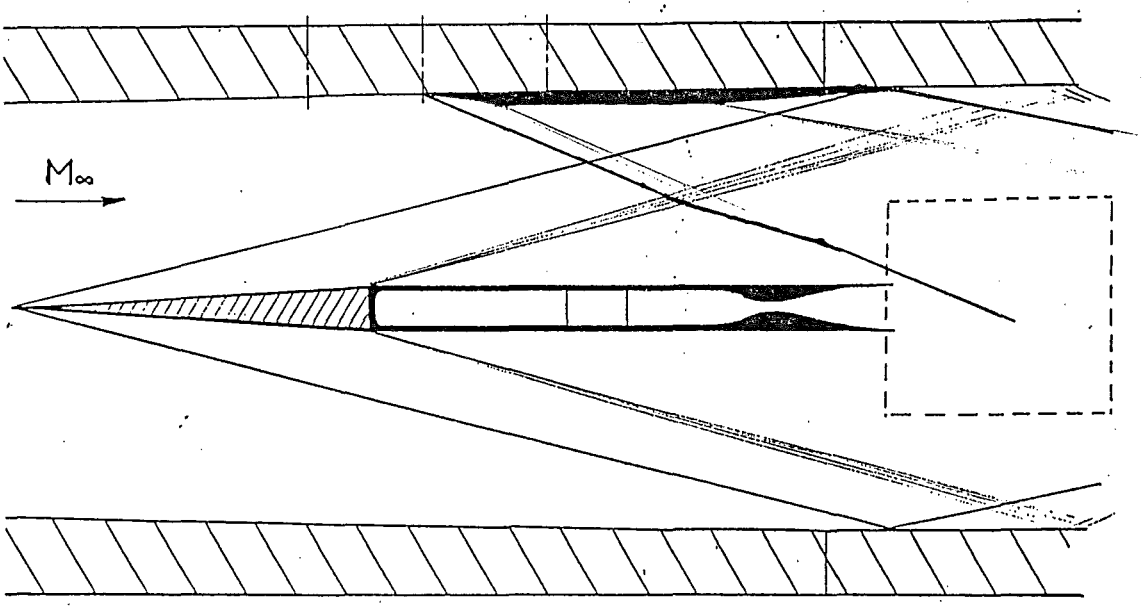


Figure 11. Schematic of set-up for shear layer under disturbance.

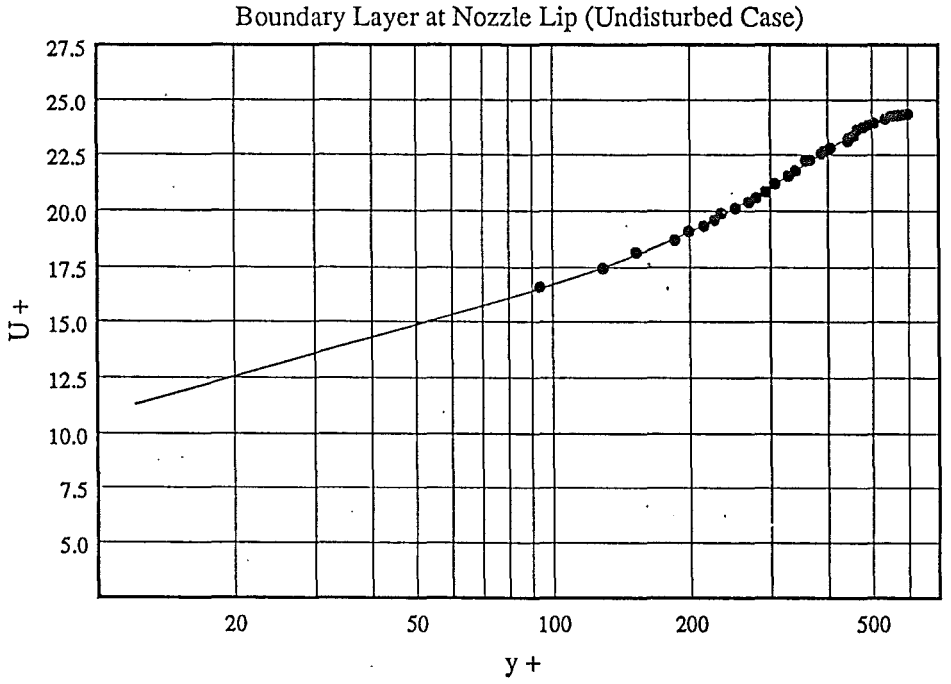


| | | |
|---|---|---|
| Mach Number | $M_\infty$ | 4.90 |
| Free Stream Total Pressure | $Pt_\infty$ | 300 (psia) |
| Free Stream Total Temperature | $Tt_\infty$ | 349.5 (°K) |
| B. L. thickness | $\delta$ | 0.5569 (cm) |
| Displacement thickness | $\delta^*$ | 0.2461 (cm) |
| Momentum thickness | $\theta$ | 0.020 (cm) |
| Shape factor | H | 12.1 |
| Reynold's number | $Re_\theta$ | 9.50 E+03 |
| Unit Reynold's number | Re/m | 4.67 E+07 ($m^{-1}$) |
| Wake parameter | $\Pi$ | 0.769 |
| Skin friction Coeff. | $C_f$ | 0.00091 |
| Mixing Convective Mach No. | $M_c$ | 0.384 |

Figure 12. Mach 5 boundary layer $u^+ - y^+$ velocity profile and free stream properties (Undisturbed Case).

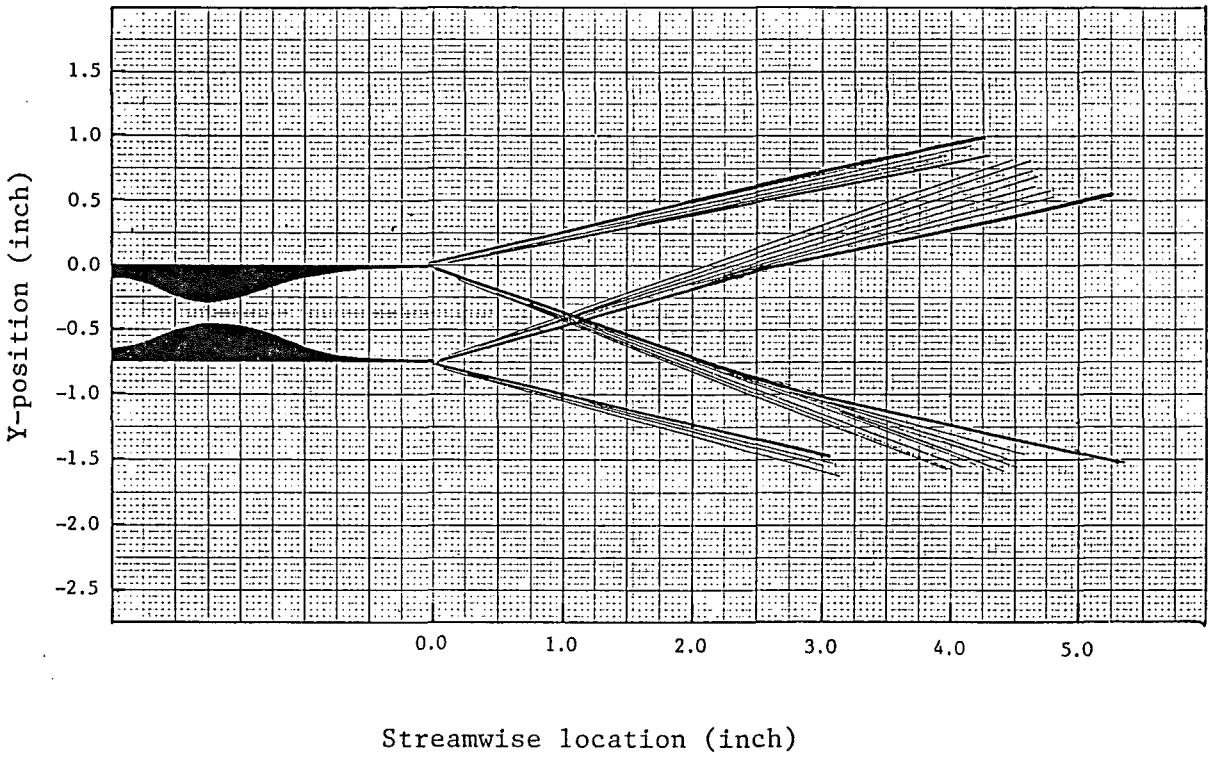


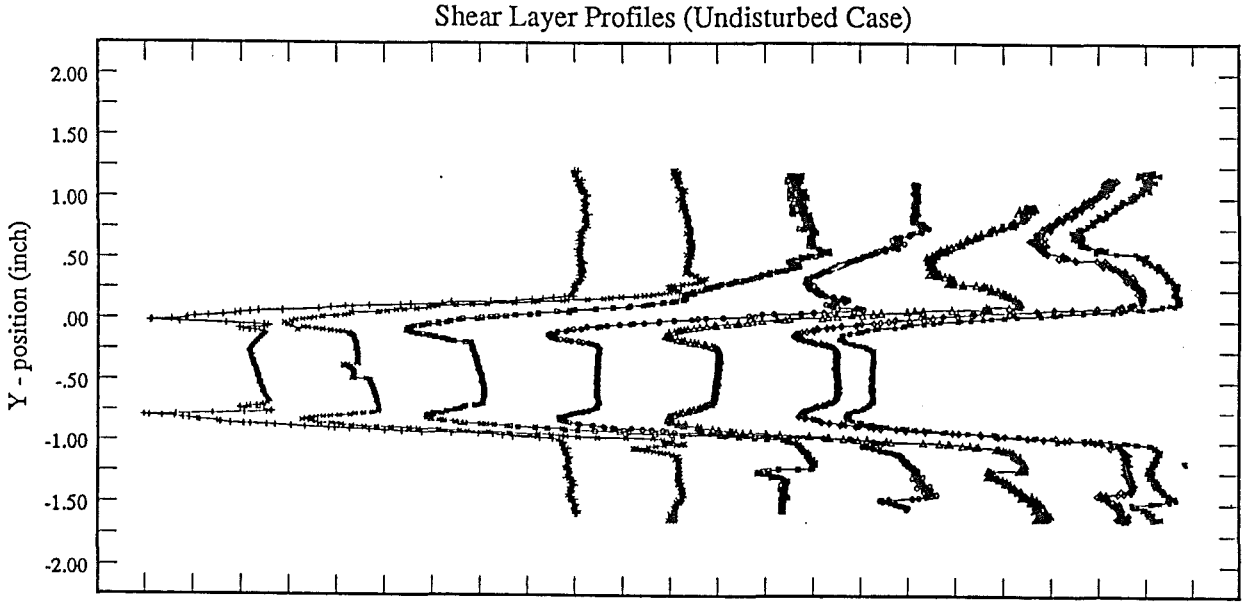


Figure 13. Shear layer pitot pressure profiles at several streamwise position and wave patterns in the shear layer flow field (Undisturbed Case).

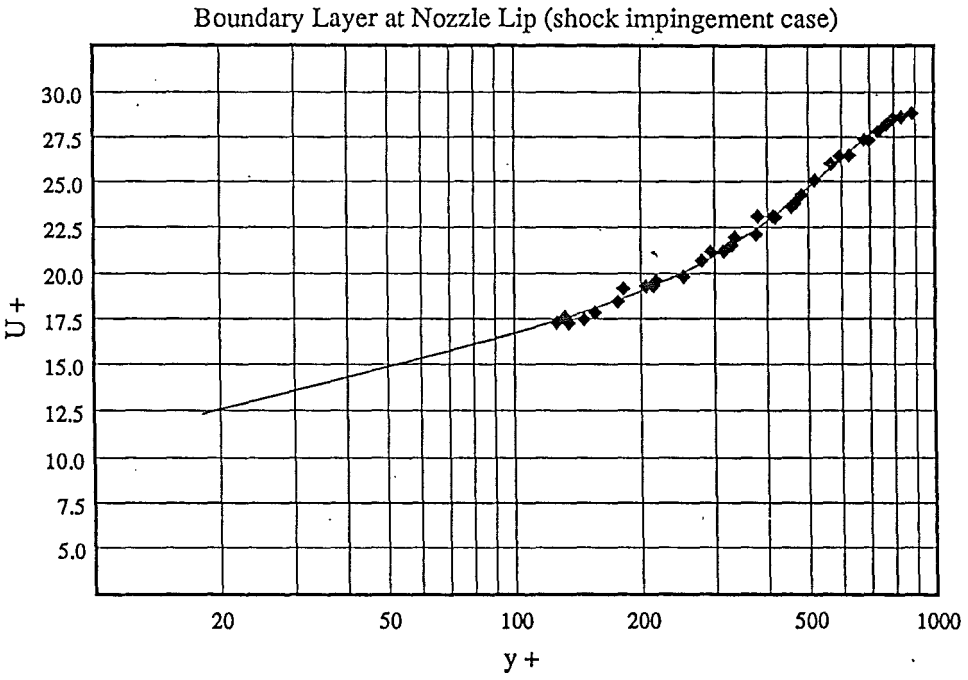


| | | |
|---|---|---|
| Mach Number | $M_\infty$ | 4.30 |
| Free Stream Total Pressure | $Pt_\infty$ | 290 (psia) |
| Free Stream Total Temperature | $Tt_\infty$ | 349.5 (°K) |
| B. L. thickness | $\delta$ | 0.559 (cm) |
| Displacement thickness | $\delta^*$ | 0.257 (cm) |
| Momentum thickness | $\theta$ | 0.0258 (cm) |
| Shape factor | H | 9.96 |
| Reynold's number | $Re_\theta$ | 1.49 E+04 |
| Unit Reynold's number | Re/m | 5.78 E+07 ($m^{-1}$) |
| Wake parameter | $\Pi$ | 1.46 |
| Skin friction Coeff. | $C_f$ | 0.00078 |
| Mixing Convective Mach No. | $M_C$ | 0.318 |

Figure 14. Mach 5 boundary layer $u^+ - y^+$ velocity profile and free stream properties (Disturbed Case: shock/ B.L. at 2.5" upstream of lip).

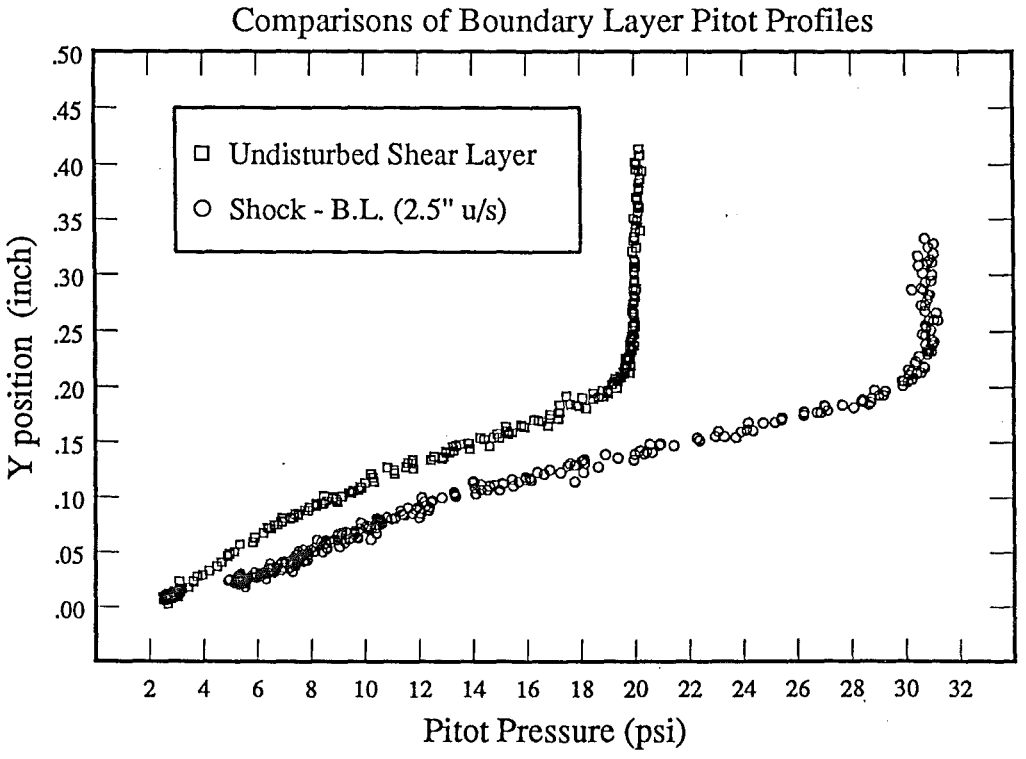


Figure 15. Comparisons of boundary layer pitot pressure profiles at nozzle lip for the undisturbed and disturbed case.

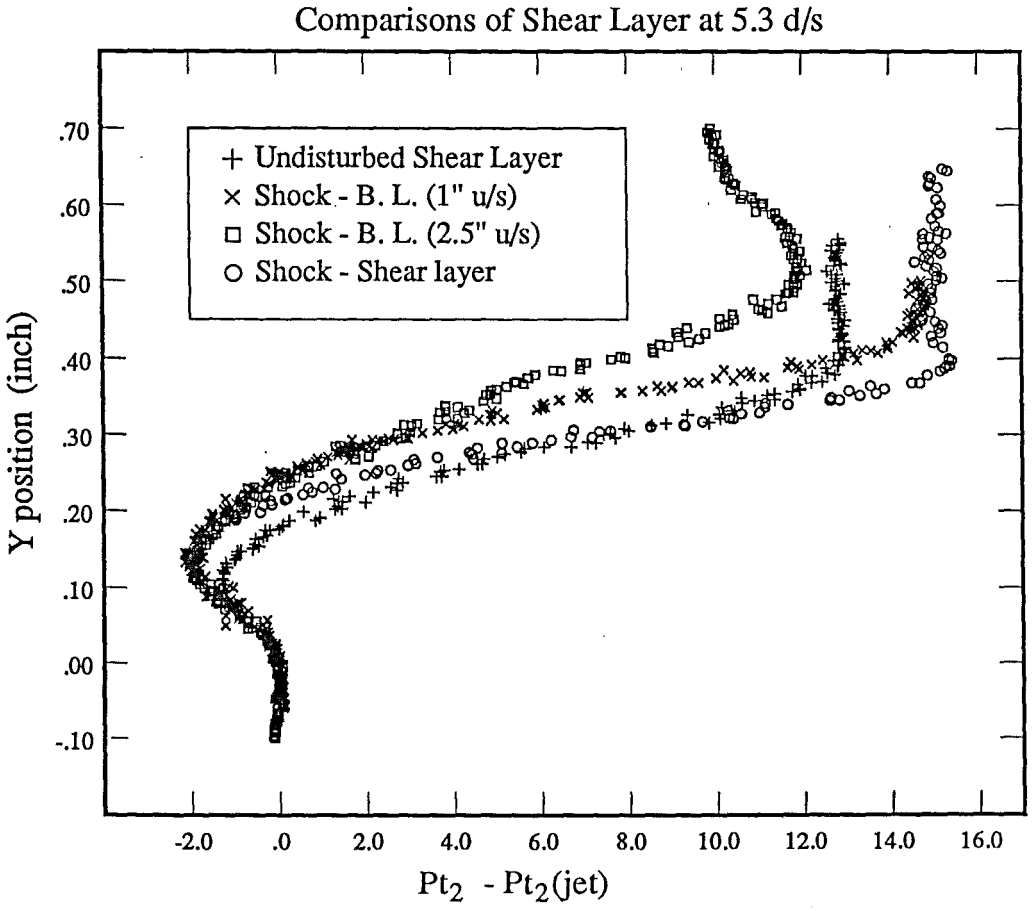


Figure 16. Comparisons of shear layer pitot pressure profiles at 5.3" downstream of nozzle lip with/without disturbances.